corrosion and materials degradation

MDPI

Supplementary Materials

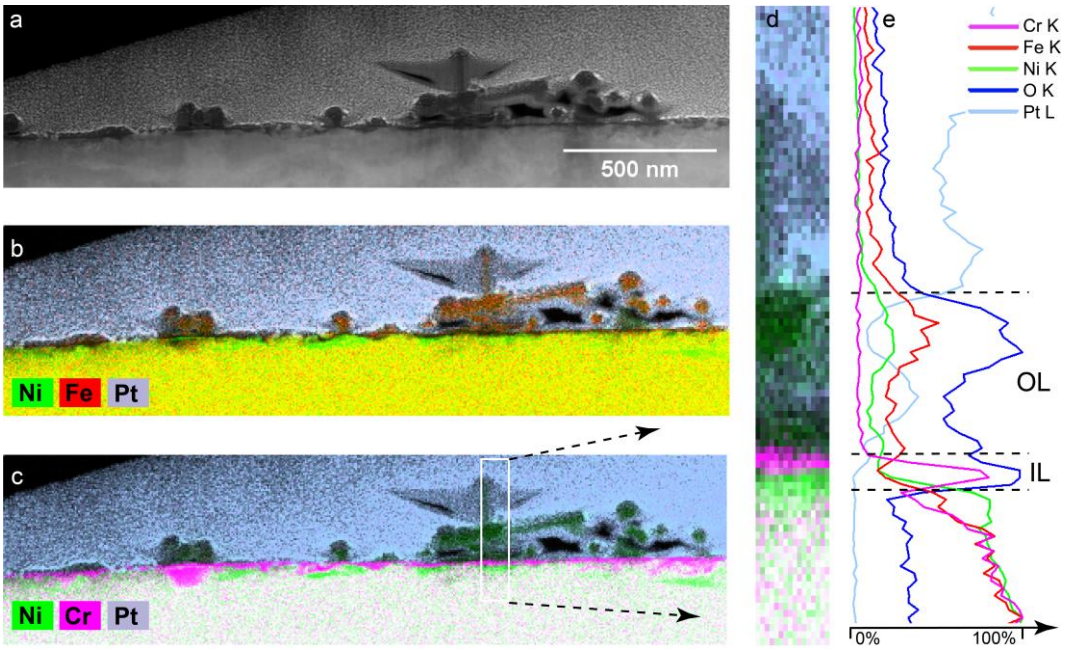

Figure S1. (a) Dark-field, cross-sectional image of Alloy 600 polarized at -695 mV in PWR PW with no zinc. (b) EDS map of nickel, iron, platinum. (c) EDS map of nickel, chromium, platinum. (d) EDS map of region of narrow width pictured in Figure (c). (e) Integrated intensities of elements in region of narrow width.

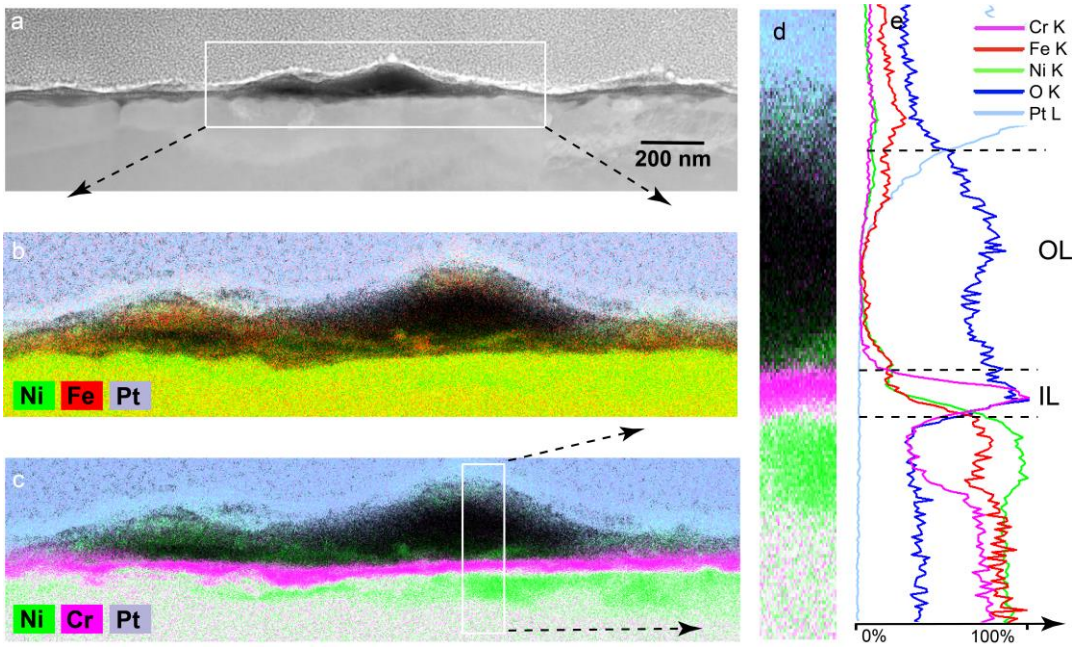

Figure S2. (a) Dark-field, cross-sectional image of Alloy 600 polarized at -223 mV in PWR PW with no zinc. (b) EDS map of nickel, iron, platinum. (c) EDS map of nickel, chromium, platinum. (d) EDS map of region of narrow width pictured in Figure (c). (e) Integrated intensities of elements in region of narrow width.

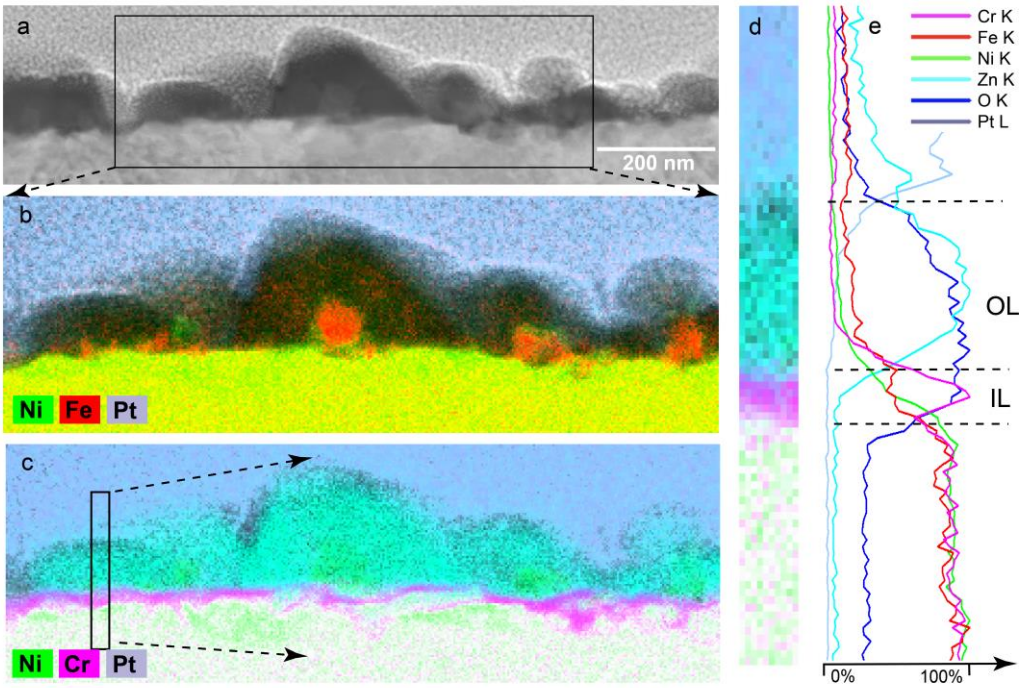

Figure S3. (a) Dark-field, cross-sectional image of Alloy 600 polarized at -700 mV in PWR PW with 100 pp zinc. (b) EDS map of nickel, iron, platinum. (c) EDS map of nickel, chromium, platinum. (d) EDS map of region of narrow width pictured in Figure (c). (e) Integrated intensities of elements in region of narrow width.

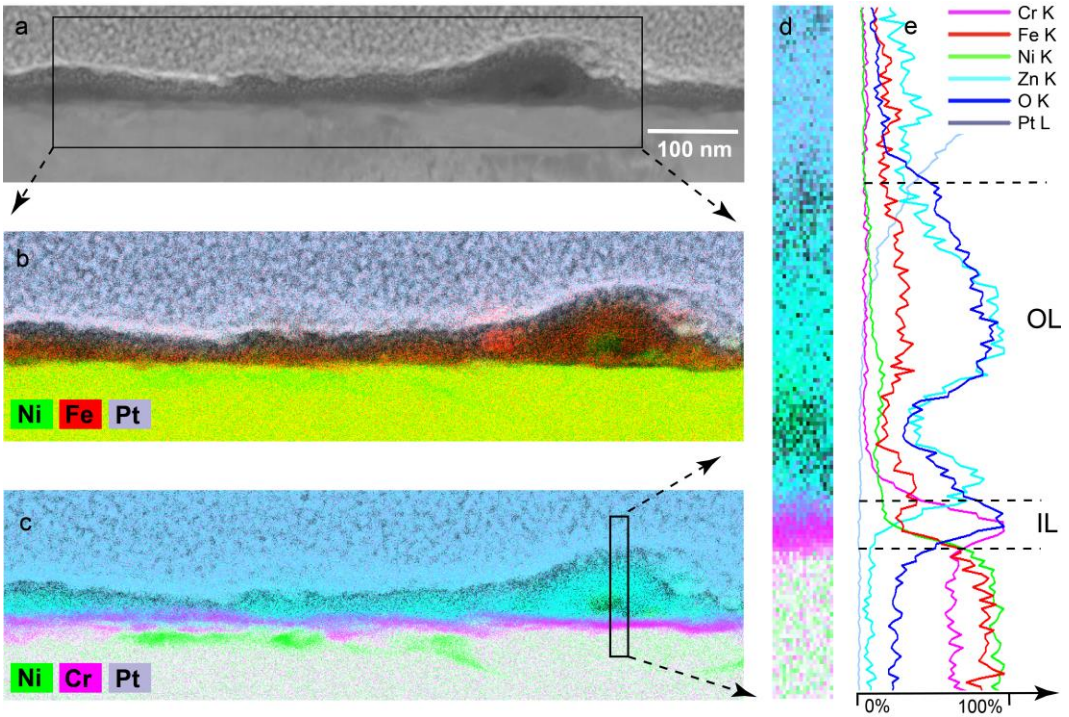

Figure S4. (a) Dark-field, cross-sectional image of Alloy 600 polarized at -223 mV in PWR PW with 100 ppb zinc. (b) EDS map of nickel, iron, platinum. (c) EDS map of nickel, chromium, platinum. (d) EDS map of region of narrow width pictured in Figure (c). (e) Integrated intensities of elements in region of narrow width.

Table S1. Composition comparison of Cr-rich layers and alloy substrates formed with and without zinc at -550mV, in atomic percent; slash separates the two samples.

At. % No-Zn/With-Zn	O	Cr	Fe	Ni	Zn	Pt
Cr-rich layer only	36/35	17/16	5/6	42/42	<1/<1	<1/<1
Deep in NiFeCr substrate	8/4	14/15	8/8	70/73	<1/<1	<1/<1
Substrate composition reported in the text:		15.4	8.5	76.1		

Table 2. Compositions of OLs near -700 mV, -550 mV and -223 mV with and without 100 ppb zinc.

Outer Layer particles/layer No Zn -700mV atomic percent

Spectrum	O	Cr	Fe	Ni
Map 1 Dec 6 2016 part	59.0	1.7	7.3	32.0
Map 2 Dec 6 2016 part	55.6	2.5	8.1	33.7
Map 3 Dec 6 2016 part	44.3	2.9	9.3	43.4
Map 4 Dec 6 2016 part	68.9	1.6	5.5	24.0
Mean value:	57.0	2.2	7.6	33.3
Sigma:	10.1	0.6	1.6	8.0
Sigma mean:	5.1	0.3	0.8	4.0

Outer Layer particles/layer No Zn -550mV atomic percent

Spectrum	O	Cr	Fe	Ni
Map 5 Dec 6 2016 part	63.2	1.4	2.8	32.6
Map 6 Dec 6 2016 part	61.4	2.0	3.2	33.3
Map 7 Dec 6 2016 part	54.0	2.5	4.1	39.4
Mean value:	59.5	2.0	3.4	35.1
Sigma:	4.9	0.6	0.7	3.8
Sigma mean:	2.8	0.3	0.4	2.2

Outer Layer particles/layer No Zn -223mV atomic percent

Spectrum	O	Cr	Fe	Ni
Map 1 May 1 2017 part	43.1	8.4	6.6	41.9
Map 2 May 2 2017 part	44.9	2.6	16.0	36.4
Map 3 May 2 2017 layer	74.9	1.9	3.7	19.6
Map 4 May 2 2017 layer	43.6	3.8	10.5	42.2
Map 5 May 2 2017 layer	60.4	1.5	7.4	30.7
Mean value:	53.4	3.6	8.8	34.1
Sigma:	14.0	2.8	4.7	9.4
Sigma mean:	6.3	1.3	2.1	4.2

Outer Layer particles With Zn -700mV atomic percent

Spectrum	O	Cr	Fe	Ni	Cu	Zn
Map 2 Sep 1 2016 outer particles	59.2	1.5	4.4	19.3	0.0	15.6
Map 3 Sep 1 2016 outer particles p	56.8	1.9	4.8	20.7	0.0	15.8
Map 4 Sep 1 2016 Outer particles p	56.7	0.8	5.0	20.4	0.0	17.1
Map 1 Sep1 2016 outer particles p	70.1	0.2	3.1	15.5	0.0	11.1
Mean value:	60.7	1.1	4.3	19.0	0.0	14.9
Sigma:	6.4	0.7	0.8	2.4	0.0	2.6
Sigma mean:	3.2	0.4	0.4	1.2	0.0	1.3

Outer Layer particles/layer With Zn -550mV atomic percent

Spectrum	O	Cr	Fe	Ni	Cu	Zn
Map 1 April 4 2017 outer layer	75.4	0.1	5.1	16.0	0.0	3.4
Map 2 April 4 2017 outer layer	66.6	0.2	6.6	21.1	0.0	5.5
Map 3 April 4 2017 outer particle one	78.4	0.1	2.0	8.8	0.0	10.6
Mean value:	73.5	0.1	4.5	15.3	0.0	6.5
Sigma:	6.1	0.0	2.4	6.2	0.0	3.7
Sigma mean:	3.5	0.0	1.4	3.6	0.0	2.1

Outer Layer particles/layer With Zn -223mV atomic percent

Spectrum	O	Cr	Fe	Ni	Cu	Zn
Map 1 August 18 2016 outer layer	65.4	5.2	5.0	15.3	0.0	9.0
Map 2 August 18 2016 outer layer	65.4	2.3	5.8	15.8	0.0	10.6
Map 3 August 18 2016 outer layer	57.7	4.3	6.5	18.8	0.0	12.7
Map 4 August 18 2016 outer layer	44.7	7.9	8.0	26.5	0.0	12.9
Mean value:	58.3	4.9	6.3	19.1	0.0	11.3
Sigma:	9.8	2.3	1.3	5.2	0.0	1.9
Sigma mean:	4.9	1.2	0.6	2.6	0.0	0.9

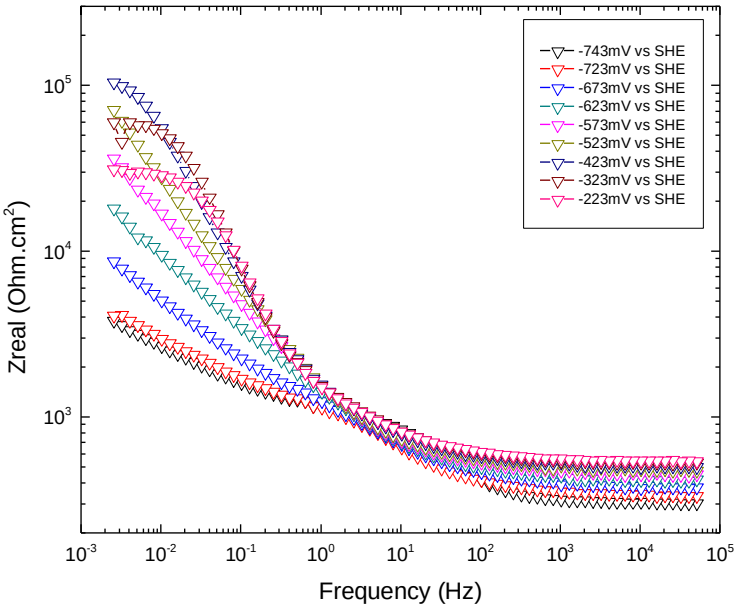

Figure S5. Influence of potential on the real component of impedance of Alloy 600 in PWR PW with no Zn.

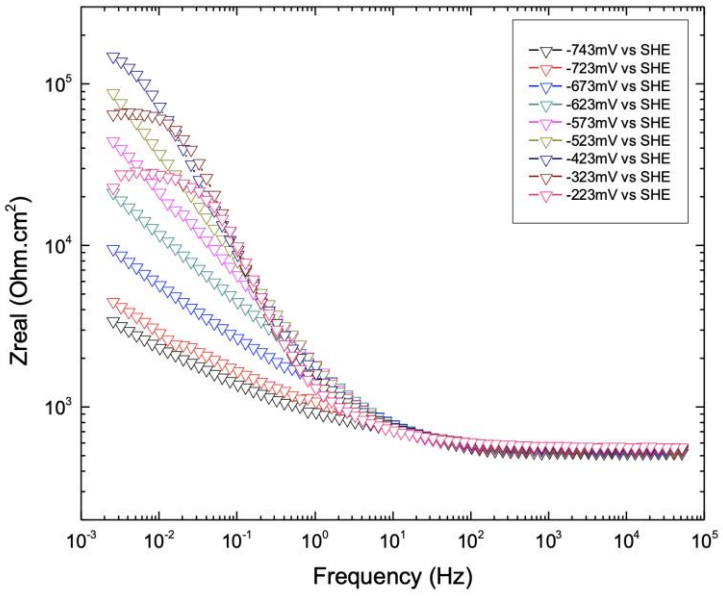

Figure S6. Influence of potential on the real component of impedance of Alloy 600 in PWR PW with Zn.

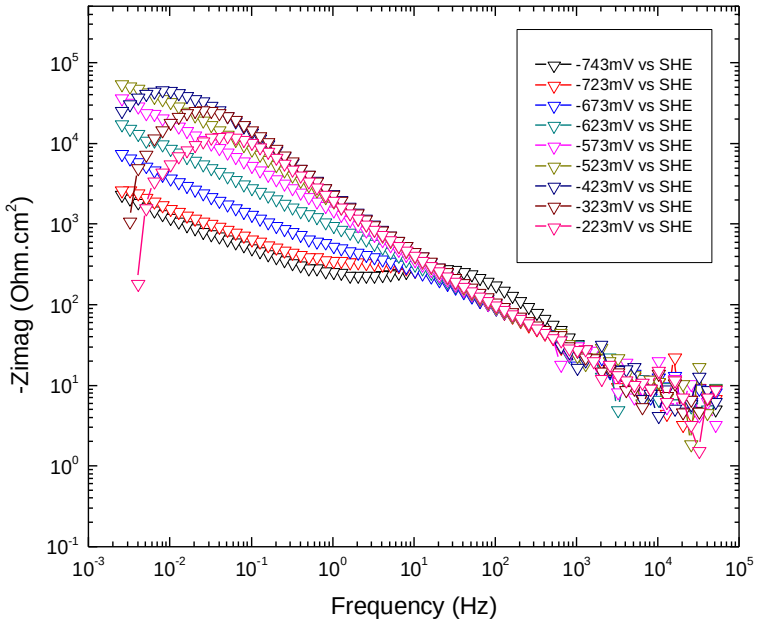

Figure S7. Influence of potential on the imaginary component of impedance of Alloy 600 in PWR PW with no Zn.

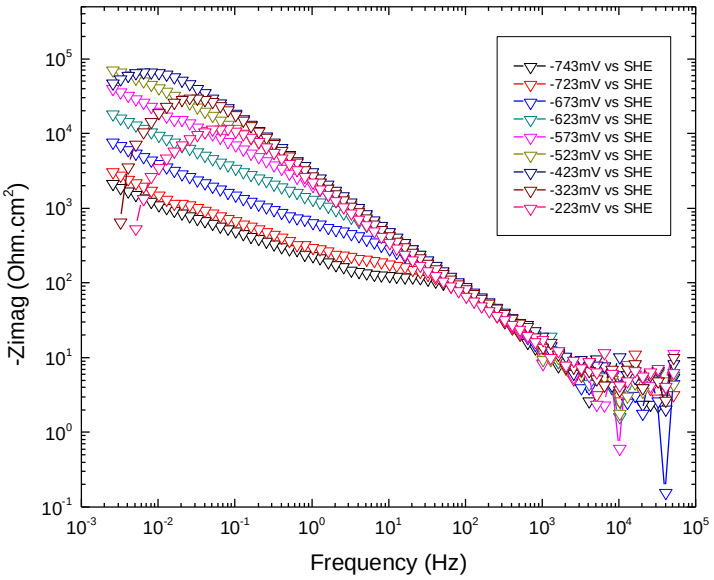

Figure S8. Influence of potential on the imaginary component of impedance of Alloy 600 in PWR PW with Zn.

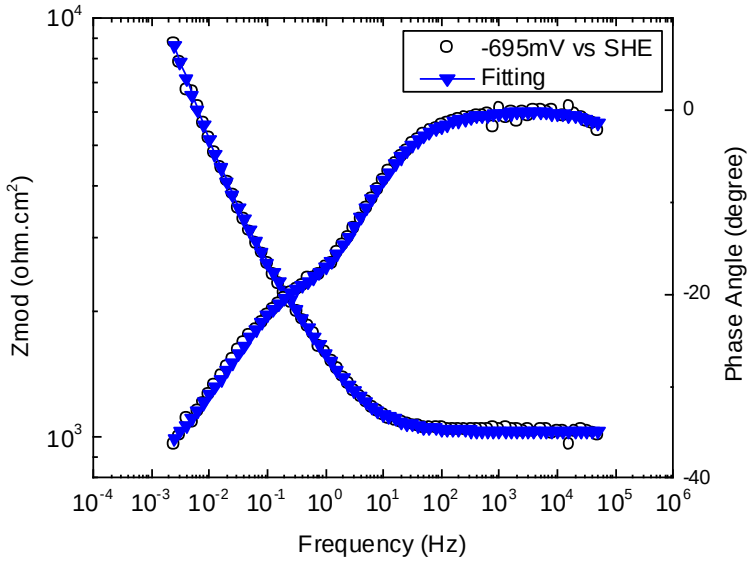

Figure S9. Fitting the modulus and phase angle of the impedance of the EC to the measured impedance at -695 mV in PWR PW without zinc. After EIS, sample's surface film was examined by SEM and TEM.

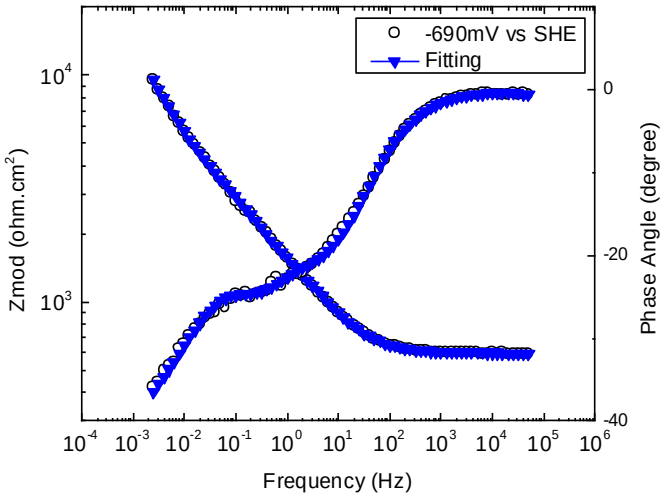

Figure S10. Fitting the modulus and phase angle of the impedance of the EC to the measured impedance at -690 mV in PWR PW with 100 ppb zinc. After EIS, sample's surface film was examined by SEM and TEM.

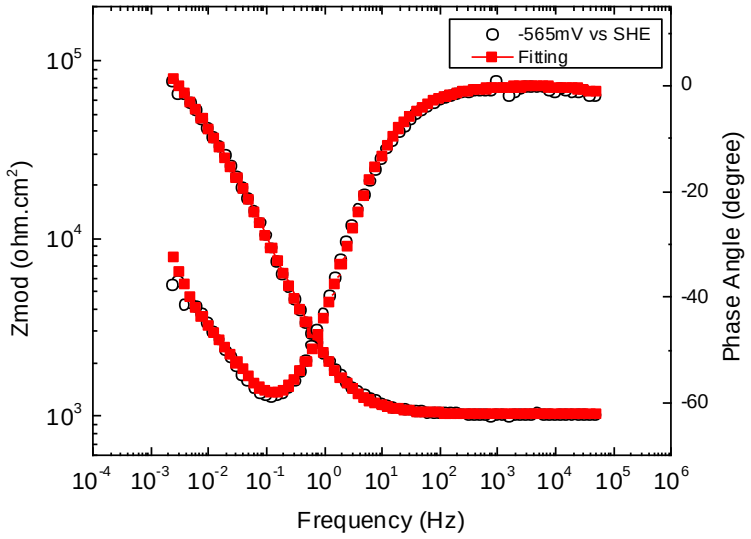

Figure S11. Fitting the modulus and phase angle of the impedance of the EC to the measured impedance at -565 mV in PWR PW without zinc. After EIS, sample's surface film was examined by SEM and TEM.

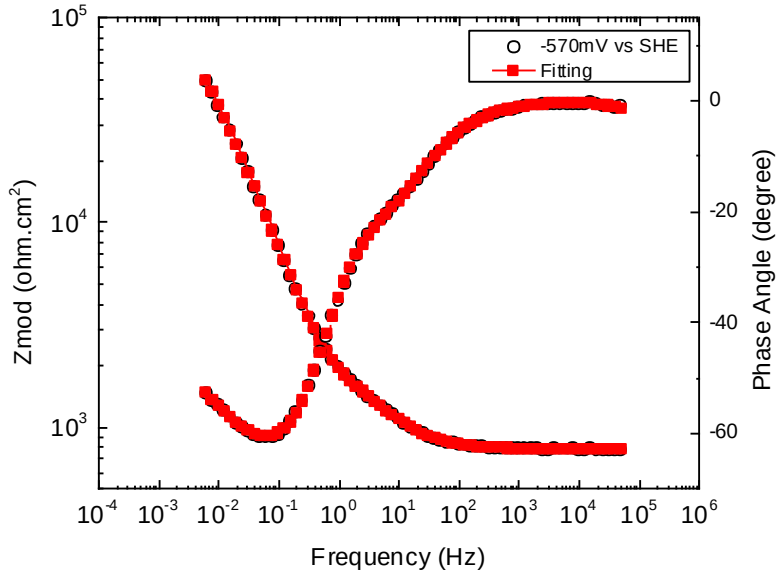

Figure S12. Fitting the modulus and phase angle of the impedance of the EC to the measured impedance at -570 mV in PWR PW with 100 ppb zinc. After EIS, sample's surface film was examined by SEM and TEM.

Comments about Figures SI-13(a,b,c) are presented after the figures.

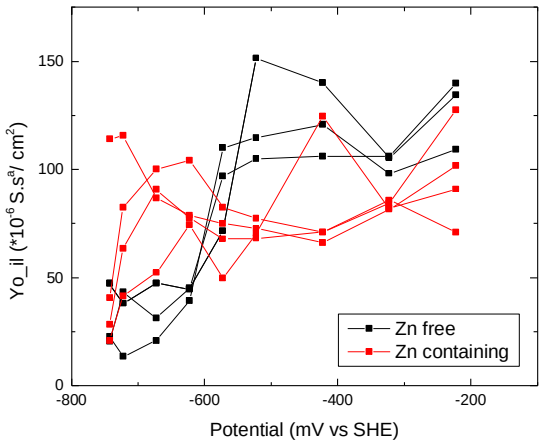

Figure S13. a. Frequency-independent factor of the impedance of the constant phase element of the IL.

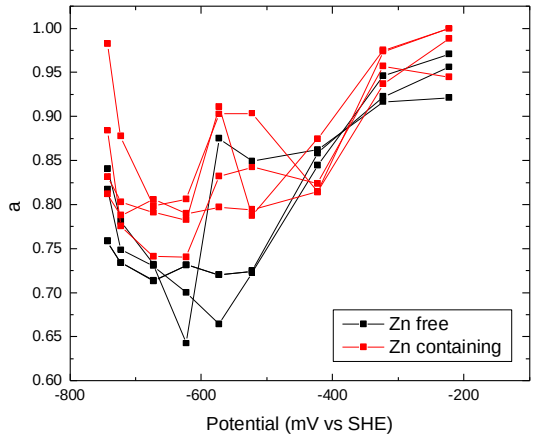

Figure S13. b. Exponent of frequency of the impedance of the constant phase element of the IL.

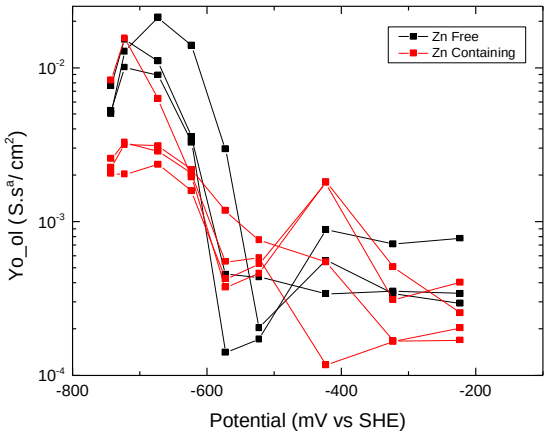

Figure S13. c. Frequency-independent factor of the impedance of the constant phase element of the OL.

Figures S13(a,b,c) It is unlikely that the capacitive elements of the ECs can account for zinc's effect on the oxidation rate, but we considered the capacitive elements for the sake of completeness.

The impedance of a constant phase element (CPE) equals $Y_o \bullet (\text{frequency})^{-a}$. The results presented in Figures SI-13(a,b,c) indicate that zinc affected the values of Y_{il}, a_{il}, and Y_{ol}. Zinc also affected the value of R_R. The biggest effect of zinc was on the value of R_R, as indicated in Figure 18c. For example, consider the EIS at -623 mV, which was in the middle of the range of potential in which R_{ox} was constant in the Zn-test and which includes steady-state values of the corrosion potential of Alloy 600 in PWR PW (≈ -800 mV <-> -700 mV). The values of the components of the EC in the Zn-tests and No-Zn-tests at -623 mV were as follows:

1) From Figure SI-13a: $Y_{il}{}^{(withZn)} \approx 5x10^{-6}$ which is < $Y_{il}{}^{(No\text{-}Zn)} \approx 30x10\text{-}6$; and from Figure SI-13b: $a_{il}{}^{(withZn)} \approx 0.8$, which is > $a_{il}{}^{(No\text{-}Zn)} \approx 0.7$
2) From Figure 18c: $R_R{}^{(withZn)} \approx 3000$ ohm•cm^2 >> $R_R{}^{(No\text{-}Zn)} \approx 200$ ohm•cm^2.
3) From Figure SI-13c: $Y_{ol}{}^{(withZn)} \approx 3x10^{-3} < Y_{ol}{}^{(No\text{-}Zn)} \approx 1x10^{-2}$

By far, the largest effect of Zn was on the value of R_R, which is 15 times greater for the Zn-test than the No-Zn test. Accordingly, R_R was a main focus of the Discussion section.